Resonant and nonresonant contributions to the weak $D \to V l^+ l^-$ decays

S. Fajfer and S. Prelovšek
J. Stefan Institute, Jamova 39, P.O. Box 300, 1001 Ljubljana, Slovenia

P. Singer
Department of Physics, Technion—Israel Institute of Technology, Haifa 32000, Israel
(Received 26 May 1998; published 7 October 1998)

The Cabibbo suppressed decays $D \to V l^+ l^-$ (V is light vector meson) present in principle the opportunity to observe the short distance FCNC transition $c \to u l^+ l^-$, which is sensitive to physics beyond the standard model. We analyze these as well as the Cabibbo allowed $D \to V l^+ l^-$ decays within the standard model, where in addition to the short distance dynamics also the long distance dynamics is present. The long distance contribution is induced by the effective nonleptonic weak Lagrangian accompanied by the emission of a virtual photon, which occurs resonantly via conversion from a vector meson ρ^0, ω or ϕ or nonresonantly as direct emission from a D meson. We calculate the branching ratios for all $D \to V l^+ l^-$ decays using the model, which combines heavy quark symmetry and chiral perturbation theory. The short distance contribution due to $c \to u l^+ l^-$ transition, which is present only in the Cabibbo suppressed decays, is found to be three orders of magnitude smaller than the long distance contribution. The branching ratios well above 10^{-7} for Cabibbo suppressed decays could signal new physics. The most frequent decays are the Cabibbo allowed decays, which are expected at the rates, that are not much lower than the present experimental upper limit: $D_s^+ \to \rho^+ \mu^+ \mu^-$ is expected at the branching ratio of approximately 3×10^{-5}, while $D^0 \to \bar{K}^{*0} \mu^+ \mu^-$ is expected at 1.7×10^{-6}. [S0556-2821(98)06121-9]

PACS number(s): 13.20.Fc, 12.39.Hg, 12.40.Vv, 13.25.Ft

I. INTRODUCTION

In the charm sector phenomena such as $D^0 - \bar{D}^0$ mixing, CP violation and rare decay probabilities are small, which makes them good candidates as probes for new physics with small background from the standard model [1–3]. In particular, decays of type $D \to X l^+ l^-$ were singled out [4–6] as a possible good window to non-standard contributions of the flavor-changing neutral transition (FCNC) $c \to u l^+ l^-$, at the 10^{-7} level for the branching ratios. This suggestion was prompted by the smallness of the short-distance (SD) $c \to u l^+ l^-$ contribution within the standard model, which leads [4,6] to a branching ratio of only 10^{-9} for the inclusive process. Although QCD corrections to this process have not been calculated in detail yet, these are not expected to affect significantly the size of the $c \to u l^+ l^-$ amplitude, as explained in the next section. Accordingly, one expects the hadronic exclusive decays induced by this SD transition to occur with branching ratios of the order of 10^{-10}.

Further studies, which have considered the long-distance (LD) contribution to $D \to P l^+ l^-$ transitions (P is light pseudoscalar) [6,7] have concluded that these are larger than SD ones. The analysis of the LD contributions in $D^{+,0} \to \pi^{+,0} l^+ l^-$ [7] has shown these modes are expected to lead to branching ratios of the order of 10^{-6} in the resonance region and a few times 10^{-7} in the nonresonant region, thus practically invalidating their use for observing the $c \to u l^+ l^-$ transition within the standard model.

A similar situation holds in the case of $D \to V \gamma$ ($D \to P \gamma$ is forbidden), where long distance effects [8–10] cause these modes to have branching ratios in the $10^{-7} - 10^{-4}$ range. On the other hand, the SD component due to the magnetic electroweak penguin transition $c \to u \gamma$ is Glashow-Yliopoulus-Meiani (GIM) suppressed and does not reach beyond the 10^{-9} range at most, despite being considerably enhanced by QCD corrections [8,11]. Thus, here again the LD effects mask the contribution of the SD $c \to u \gamma$ loop, except for very special circumstances, which were pointed out recently [9,12].

We analyze LD and SD contributions to all $D \to V l^+ l^-$ decays within the standard model. The SD contribution due to $c \to u l^+ l^-$ is present only in the Cabibbo suppressed decays $D^0 \to \rho^0 l^+ l^-$, $D^0 \to \omega l^+ l^-$ $D^0 \to \phi l^+ l^-$, $D^+ \to \rho^+ l^+ l^-$ and $D_s^+ \to K^{*+} l^+ l^-$. Our results should provide the appropriate theoretical background against which possible signals of new physics are searched for in these decays. Motivated by the experimental searches, we analyze also the Cabibbo allowed decays ($D^0 \to K^{*0} l^+ l^-$ and $D_s^+ \to \rho^+ l^+ l^-$), which are the best candidates for their early detection, and the doubly Cabibbo suppressed decays ($D^+ \to K^{*+} l^+ l^-$ and $D^0 \to K^{*0} l^+ l^-$). Here the signals from new physics are not expected from the theoretical models usually considered.

On the experimental side, so far there are only upper bounds on the branching ratios of $D \to V l^+ l^-$ decays from E653 Collaboration and CLEO Collaboration [13,14], in the range $10^{-3} - 10^{-4}$, but these are expected to improve in the future.

In Sec. II we present the details of our approach and we define the approximations used. In Sec. III we give the results of our calculations and we summarize in Sec. IV.

II. MODEL DESCRIPTION

A. Long distance contributions

In this subsection we present the general framework used for calculating the long distance amplitudes, while the details

of the model employed are given in Sec. II C. The long distance contribution in $D\to Vl^+l^-$ decays is due to the effective nonleptonic weak Lagrangian, which induces the weak transition between the initial and final hadronic state. The weak transition has to be accompanied by the emission of a virtual photon, which finally decays into a lepton antilepton pair. The effective nonleptonic weak Lagrangian responsible for charm meson decays is

$$\mathcal{L}_{LD}=-\frac{G_F}{\sqrt{2}}V_{uq_i}V^*_{cq_j}[a_1(\bar{u}q_i)^\mu(\bar{q}_jc)_\mu+a_2(\bar{u}c)_\mu(\bar{q}_jq_i)^\mu], \tag{1}$$

where $(\bar{\psi}_1\psi_2)^\mu\equiv\bar{\psi}_1\gamma^\mu(1-\gamma^5)\psi_2$, $q_{i,j}$ represent the fields of d or s quarks, V_{ij} are the Cabibbo-Kobayashi-Maskawa (CKM) matrix elements and G_F is the Fermi constant. In our calculation we use $a_1=1.26$ and $a_2=-0.55$ as found in [15], from an extensive application of Eq. (1) to the study of nonleptonic D decays.

The virtual photon emission from the hadronic states is taken in our approach to proceed through two different mechanisms:

(i) In the *nonresonant mechanism* the photon is emitted directly from the initial D state.

(ii) In the *resonant mechanism*, apart from the final vector meson V, an additional neutral vector meson V_0 is produced, which converts to a photon through vector meson dominance (VMD). In this case, a nonleptonic weak decay $D\to VV_0$ is followed by the transition $V_0\to\gamma^*\to l^+l^-$, where V_0 is a short-lived vector meson ρ^0, ω or ϕ.

The evaluation of the matrix elements of the product of two currents (1) requires nonperturbative techniques and we are forced to use some approximation. We have undertaken to use systematically the factorization approximation, where the matrix element of the product of two currents is approximated by

$$\begin{aligned}\langle V\gamma|(\bar{q}_iq_j)^\mu(\bar{q}_kc)_\mu|D\rangle=&\langle V|(\bar{q}_iq_j)^\mu|0\rangle\langle\gamma|(\bar{q}_kc)_\mu|D\rangle\\&+\langle\gamma|(\bar{q}_iq_j)^\mu|0\rangle\langle V|(\bar{q}_kc)_\mu|D\rangle\\&+\langle V\gamma|(\bar{q}_iq_j)^\mu|0\rangle\langle 0|(\bar{q}_kc)_\mu|D\rangle.\end{aligned} \tag{2}$$

The first two terms are the spectator contributions, in the following denoted by $A_{Spec,\gamma}$ and $A_{Spec,V}$, respectively, and the third term is the weak annihilation contribution, denoted by A_{Annih}. Here γ denotes the virtual photon.

To calculate the matrix elements in Eq. (2) we use the hybrid model, which combines heavy quark effective theory (HQET) and chiral Lagrangian [16–18] and has been successfully employed already for D meson decays in several papers [16–26]. A very detailed description of the hybrid model and its previous applications is given in [18].

The relevant hadronic degrees of freedom for the present calculation are heavy pseudoscalar (D) and vector mesons (D^*) and light pseudoscalar (P) and vector (V) mesons. Within this approach the diagrams that contribute to the amplitudes $A_{Spec,\gamma}$, $A_{Spec,V}$ and A_{Annih} (2) are shown in Figs. 1(a), 1(b) and 1(c), respectively. Different diagrams in Fig. 1 are denoted by the roman numbers from I–VIII. Diagrams III and IV in Fig. 1 represent nonresonant contribution (mechanism (i)). All the remaining diagrams, which proceed through the intermediate short-lived vector meson V_0 (ρ, ω and ϕ), represent the *resonant contribution* (mechanism (ii)). The resonant amplitude is represented in the whole q^2 region by the Breit-Wigner vector meson propagator. (q is the sum of lepton and antilepton momenta.) In the regions of q^2 far away from m^2_{V0}, the resonant amplitude is given therefore solely by the tail of the Breit-Wigner vector meson propagator. The square in each diagram of Fig. 1 denotes the weak transition due to the effective Lagrangian $\mathcal{L}_{LD}$ (1). This Lagrangian contains a product of two left handed quark currents $(\bar{q}_kq_l)^\mu$, each denoted by a dot on Fig. 1. The left handed currents will be expressed in terms of the relevant hadronic degrees of freedom: D, D^*, P and V. In our notation the hadronic current J_2 in diagram II, for example, creates a V meson, while the hadronic current J_1 annihilates D and creates V_0 at the same time.

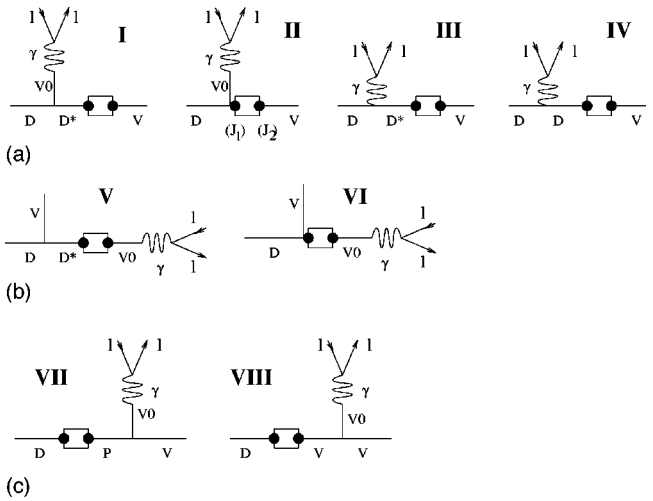

FIG. 1. Skeleton diagrams of various *long distance contributions* to the decay $D\to Vl^+l^-$ resulting from Eq. (2). The spectator diagrams of type $A_{Spec,\gamma}$ [see Eq. (2)] are shown in Fig. 1(a), the spectator diagrams of type $A_{Spec,V}$ are shown in Fig. 1(b) and the weak annihilation diagrams A_{Annih} are shown in Fig. 1(c). Different diagrams are denoted by the roman numbers I–VIII. The square in each diagram denotes the weak transition due to the long distance Lagrangian $\mathcal{L}_{LD}$ [Eq. (1)]. This Lagrangian contains a product of two weak currents, each denoted by a dot.

In the model we use, there is no contribution of J/Ψ or other $\bar{c}c$ excited states. The contribution that would arise by the exchange of this mesons is effectively described by diagram III of Fig. 1, where $\bar{c}c$ exchange is ''hidden'' in the $DD^*\gamma$ coupling. The alternative approach of a direct $\bar{c}c$ exchange would require the knowledge of their couplings to photons over a wide region of q^2, of which one has only rudimentary knowledge [27].

B. Short distance contributions due to $c\to ul^+l^-$

In addition to long distance dynamics, the Cabibbo suppressed decays $D^0\to\rho^0l^+l^-$, $D^0\to\omega l^+l^-$, $D^0\to\phi l^+l^-$,

$D^+ \to \rho^+ l^+ l^-$ and $D_s^+ \to K^{*+} l^+ l^-$ can also be driven by the short distance $c \to u l^+ l^-$ transition. The short distance part in $D \to V l^+ l^-$ decays will turn out in general to be much smaller than the long distance part. However, we shall find that in the case of $D^0 \to \rho^0(\omega) l^+ l^-$ the short distance part is of the same order of magnitude as the nonresonant part of the long distance contribution. In this subsection we estimate the size of the short distance amplitudes, which is *nonresonant* in its nature.

The effective Lagrangian for FCNC transition $c \to u l^+ l^-$ arises from WW exchange box diagrams and Z and γ^* penguin operators [4]. It has been obtained using the similar results for $s \to d l^+ l^-$ decay [28]

$$\mathcal{L}_{SD} = \frac{G_F}{\sqrt{2}} \frac{e^2}{16\pi^2 \sin^2\theta_W} \times \sum_{i=d,s,b} V_i [\bar{u}\gamma_\mu(1-\gamma_5)c(A_i \bar{l}\gamma^\mu(1-\gamma_5)l + B_i \bar{l}\gamma^\mu(1+\gamma_5)l) - 2im_c \sin^2\theta_W F_2^i q^\nu \bar{u}\sigma_{\mu\nu}(1+\gamma_5)c\bar{l}\gamma^\mu(1-\gamma_5)l], \tag{3}$$

where the Willson coefficients A_i, B_i and F_2^i are given in Appendix A and V_i are the CKM coefficients, $V_i = V_{ci}^* V_{ui}$. The expression (3) does not contain the QCD corrections, which have not been studied for $c \to u l^+ l^-$ decays so far. When referring to these corrections for $c \to u l^+ l^-$, one is reminded that in the case of $c \to u\gamma$ decay there is a huge QCD enhancement [8,11], which is due to the following reason: The effect of QCD is that the Wilson coefficient $c_7(m_c)$, responsible for the magnetic penguin decay $c \to u\gamma$, obtains the admixture of the other Wilson coefficients evaluated at the scale m_W in the leading order $c_i(m_W)$, $i = 1,\ldots,10$. Since $c_7(m_W)$ is extremely suppressed compared to some other Wilson coefficients $c_i(m_W)$, the resulting $c_7(m_c)$ is much bigger than $c_7(m_W)$ and a huge QCD enhancement for $c \to u\gamma$ occurs. In the $c \to u l^+ l^-$ decay on the other hand, the responsible Wilson coefficients $A(m_W)$ and $B(m_W)$, which do not contribute for the real photons, are not suppressed in the lowest order and one would not expect large QCD effects on them as one has learned from estimation of $s \to d l^+ l^-$ [29]. The coefficient of the magnetic transition $F_2(m_W)$, which is proportional to Wilson coefficient $c_7(m_W)$, indeed acquires large QCD corrections, however it is strongly suppressed in the lowest order. Since we are only interested in the rough estimation of the short distance contribution in $D \to V l^+ l^-$ and the last term in Eq. (3) is much less important than the other two for such decays [29], we neglect the last term altogether, using the approximation explained in Appendix A.

The Lagrangian $\mathcal{L}_{SD}$ (3) then gives the branching ratio for inclusive $c \to u l^+ l^-$ process

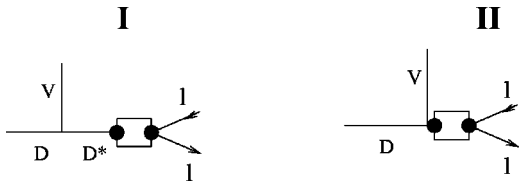

FIG. 2. Skeleton diagrams of *short distance contributions* to the decay $D \to V l^+ l^-$ due to $c \to u l^+ l^-$ transition. The squares in the diagrams denote the weak transition due to the short distance Lagrangian $\mathcal{L}_{SD}$ [Eq. (3)]. This Lagrangian contains a product of a quark and a lepton weak currents, each denoted by a dot.

$$\frac{\Gamma(c \to u l^+ l^-)}{\Gamma(D^0)} = \frac{G_F^2 m_c^5}{192\pi^3 \Gamma(D^0)} \left(\frac{\alpha}{4\pi \sin^2\theta_W}\right)^2 \times [|V_i A_i|^2 + |V_i B_i|^2] = 2.9 \times 10^{-9}.$$

To predict the exclusive amplitudes for $D \to V l^+ l^-$ induced by $\mathcal{L}_{SD}$ (3), we have to evaluate the matrix elements

$$\langle V|\bar{u}\gamma_\mu(1-\gamma_5)c|D\rangle. \tag{4}$$

We shall do this by again using the hybrid model, which is described in the next subsection. The corresponding Feynman diagrams within this approach are given in Fig. 2. The squares in the diagrams denote the weak transition due to the short distance Lagrangian $\mathcal{L}_{SD}$ (3). This Lagrangian contains a product of a quark and lepton weak currents, each denoted by a dot in Fig. 2. We remark, that these diagrams have a long distance counterpart, given by diagrams V and VI of Fig. 1, which represent the long distance $c \to u\gamma$ transition [9,29]

C. Theoretical framework: Chiral Lagrangians, heavy quark limit and vector meson dominance

Here we present the model, which we use to evaluate the matrix elements (2) and (4) needed to predict $D \to V l^+ l^-$ amplitudes. The framework we use for our treatment is that of an effective Lagrangian, which embodies two important approximate symmetries of QCD, the infinite heavy quark Q mass limit ($m_Q \to \infty$) and the chiral limit for light quarks, namely $(m_u, m_d, m_s) \to 0$. This approach, which was developed during the last few years ([16–26] and additional references quoted in [18]), has been used with a good measure of success to treat strong, electromagnetic and weak decays of D and B mesons. Obviously, an effective Lagrangian approach has also its weakness, as it involves a number of unknown coupling constants. Fortunately, the use of observed processes makes it possible to determine a good proportion of them, as detailed in this and the next subsection. Moreover, the use of form factors alleviates the limitations on the range in which the basic assumptions of the model hold to a good accuracy. The model and its various applications till now are well exposed in a recent review [18]. In the present subsection, we describe those parts which are needed for our calculation. We introduce now the strong and elec-

tromagnetic interaction Lagrangians for the heavy (hadrons containing c quark) and light (hadrons containing only light u, d and s quarks) sector and the relevant weak currents. At the end of the section we discuss the values of free parameters, that enter the Lagrangians and currents in our model. Our strong and electromagnetic Lagrangian [16–18] is invariant under heavy quark spin ($SU(2)$), chiral ($SU(3)_L \times SU(3)_R$), Lorentz, parity and $U(1)$ gauge transformation [18]. The light vector mesons are incorporated using the hidden symmetry approach [18,30]. We are aware that using (HQET), which converges very slowly in the case of c quark, presents a rather rough approximation. In spite of that, the HQET approach, which helps to reduce the number of free parameters, has been successfully applied in many D decays (e.g. [18] and references therein).

The light degrees of freedom are described by the 3×3 Hermitian matrices

$$\Pi=\begin{pmatrix} \frac{\pi^0}{\sqrt{2}}+\frac{\eta_8}{\sqrt{6}}+\frac{\eta_0}{\sqrt{3}} & \pi^+ & K^+ \\ \pi^- & -\frac{\pi^0}{\sqrt{2}}+\frac{\eta_8}{\sqrt{6}}+\frac{\eta_0}{\sqrt{3}} & K^0 \\ K^- & \bar{K}^0 & -\frac{2\eta_8}{\sqrt{6}}+\frac{\eta_0}{\sqrt{3}} \end{pmatrix} \tag{5}$$

and

$$\rho_\mu=\begin{pmatrix} \frac{\rho_\mu^0+\omega_\mu}{\sqrt{2}} & \rho_\mu^+ & K_\mu^{*+} \\ \rho_\mu^- & \frac{-\rho_\mu^0+\omega_\mu}{\sqrt{2}} & K_\mu^{*0} \\ K_\mu^{*-} & \bar{K}_\mu^{*0} & \phi_\mu \end{pmatrix}, \quad F_{\mu\nu}(\rho)=\partial_\mu\rho_\nu-\partial_\nu\rho_\mu+[\rho_\mu,\rho_\nu] \tag{6}$$

for the pseudoscalar and vector mesons, respectively. They are usually expressed through the combinations

$$u=\exp\left(\frac{i\Pi}{f}\right), \tag{7}$$

where $f\simeq f_\pi=132$ MeV is the pion pseudoscalar decay constant and

$$\hat{\rho}_\mu=i\frac{\tilde{g}_V}{\sqrt{2}}\rho_\mu, \tag{8}$$

where $\tilde{g}_V$ is fixed in the case of the exact flavor symmetry to be the VPP coupling $\tilde{g}_V=5.9$ [30].

The most general strong Lagrangian for the light mesons in the leading order of chiral perturbation theory is [30]

$$\mathcal{L}^1_{light}=-\frac{f^2}{2}\{\mathrm{Tr}(\mathcal{A}_\mu\mathcal{A}^\mu)+a\ \mathrm{Tr}[(\mathcal{V}_\mu-\hat{\rho}_\mu)^2]\} + \frac{1}{2\tilde{g}_V^2}\mathrm{Tr}[F_{\mu\nu}(\hat{\rho})F^{\mu\nu}(\hat{\rho})], \tag{9}$$

where we have introduced two currents

$$\mathcal{V}_\mu=\tfrac{1}{2}(u^\dagger D_\mu u+uD_\mu u^\dagger) \quad \text{and} \quad \mathcal{A}_\mu=\tfrac{1}{2}(u^\dagger D_\mu u-uD_\mu u^\dagger). \tag{10}$$

Demanding the Lagrangian (9) to be invariant under the local gauge transformation, corresponding to the electro-magnetic $U(1)$ transformation in QCD, we define the covariant derivatives as

$$D_\mu u=(\partial_\mu+\hat{B}_\mu)u \quad \text{and} \quad D_\mu u^\dagger=(\partial_\mu+\hat{B}_\mu)u^\dagger,$$

with $\hat{B}_\mu=ieB_\mu Q$, $Q=\mathrm{diag}(2/3,-1/3,-1/3)$ and B_μ being the photon field. The constant a (15) is in principle a free parameter. We fix it to $a=2$ [30] assuming the exact vector meson dominance, where the pseudoscalars interact with the photon only through vector mesons. With this choice, the photon-vector meson interaction given by the second term of Lagrangian (9) is

$$\mathcal{L}_{V\gamma}=-e\tilde{g}_V f^2 B_\mu\left(\rho^{0\mu}+\frac{1}{3}\omega^\mu-\frac{\sqrt{2}}{3}\phi^\mu\right). \tag{11}$$

Instead of using the exact $SU(3)$ symmetry values $\tilde{g}_V=5.9$ and $f=132$ MeV, we express the $V\gamma$ couplings in terms of the measurable quantities g_ρ, g_ω and g_ϕ defined by the matrix element of the corresponding vector current J_V^μ

$$\langle V(\epsilon_V,q)|J_V^\mu|0\rangle = g_V(q^2)\epsilon^{*\mu}(q). \quad (12)$$

In our calculation we use the values g_V given in Table II, which have been directly measured in the leptonic $V\to l^+l^-$ decays, and we make the assumption $g_V(q^2)=g_V(m_V^2)\equiv g_V$. The photon-vector meson interaction Lagrangian (11) defined through the constants g_V is

$$\mathcal{L}_{V\gamma} = -\frac{e}{\sqrt{2}}\left(g_\rho \rho^{0\mu} + \frac{g_\omega}{3}\omega^\mu - \frac{\sqrt{2}g_\phi}{3}\phi^\mu\right)B_\mu. \quad (13)$$

As far as the calculation of the amplitudes for the diagrams of Fig. 1 is concerned, the Lagrangian $\mathcal{L}_{light}$ (15) provides also the VVV vertex given by the third term in Eq. (9). The VVV vertex is present in the diagram VIII of Fig. 1, which describes the photon emission from the charged vector meson.

We need also the PVV vertex, which is present in the diagram VII of Fig. 1. This interaction term can be generated only in the next-to-leading order of chiral perturbation theory as [18]

$$\mathcal{L}^2_{light} = -4\frac{C_{VV\Pi}}{f}\epsilon^{\mu\nu\alpha\beta}\,\mathrm{Tr}(\partial_\mu\rho_\nu\partial_\alpha\rho_\beta\Pi), \quad (14)$$

where $C_{VV\Pi}$ is free parameter.

Both the heavy pseudoscalar and the heavy vector mesons are incorporated in a 4×4 matrix

$$H_a = \frac{1+\not v}{2}(P^*_{a\mu}\gamma^\mu - P_a\gamma_5),$$

$$\overline{H}_a = \gamma^0 H_a^\dagger \gamma^0 = (P^{*\dagger}_{a\mu}\gamma^\mu + P_a^\dagger\gamma_5)\frac{1+\not v}{2}, \quad (15)$$

where $a=1,2,3$ is the $SU(3)_V$ index of the light flavors and $P^*_{a\mu}$, P_a annihilate a spin 1 and spin 0 heavy meson $Q\overline{q}_a$ of velocity v, respectively. The strong and electromagnetic Lagrangian in the heavy sector have to provide us with the $DD\gamma$, $DD^*\gamma$ and DD^*V vertices. The first vertex describes the photon emission from the charged D meson and is generated in the leading order of HQET [invariant under heavy quark symmetry and $U(1)$ gauge transformation with minimal number of derivatives] as [17,18]

$$\mathcal{L}^1_{heavy} = i\,\mathrm{Tr}[H_a v^\mu(\partial_\mu + \mathcal{V}_\mu - \tfrac{2}{3}ieB_\mu)\overline{H}_a]. \quad (16)$$

The $DD^*\gamma$ and DD^*V vertices can be generated only in the next-to-leading order of the heavy quark and chiral expansion and are described by [17,18]

$$\mathcal{L}^2_{heavy} = -\lambda'\,\mathrm{Tr}[H_a\sigma_{\mu\nu}F^{\mu\nu}(B)\overline{H}_a] + i\lambda\,\mathrm{Tr}[H_a\sigma_{\mu\nu}F^{\mu\nu}(\hat\rho)_{ab}\overline{H}_b]. \quad (17)$$

The first term contributes to diagram III in Fig. 1, while the second term contributes to diagrams I and V of Fig. 1 and diagram I of Fig. 2. The λ and λ' are free parameters.

In addition to the strong and electromagnetic interaction, we have to specify the weak one. The effective weak Lagrangian responsible for the long distance contribution is given by $\mathcal{L}_{LD}$ (1) and for the short distance contribution by $\mathcal{L}_{SD}$ (3). As we deal with the probabilities for the weak decays of hadrons, we rewrite the quark weak currents in $\mathcal{L}_{LD}$ (1) and $\mathcal{L}_{SD}$ (3) in terms of hadronic degrees of freedom. The weak current $\overline{q_a}\gamma^\mu(1-\gamma^5)c$ containing a c quark and one light anti-quark $\overline{q_a}$ transforms under chiral $SU(3)_L\times SU(3)_R$ transformation as $(\overline{3}_L,1_R)$. At the hadronic level we impose the same chiral transformation and we require the current to be linear in the heavy meson fields D^a and D^{*a}_μ [16,26]

$$J^\mu_a = \tfrac{1}{2}i\alpha\,\mathrm{Tr}[\gamma^\mu(1-\gamma_5)H_b u^\dagger_{ba}] + \alpha_1\,\mathrm{Tr}[\gamma_5 H_b(\hat\rho^\mu - \mathcal{V}^\mu)_{bc}u^\dagger_{ca}] + \alpha_2\,\mathrm{Tr}[\gamma^\mu\gamma_5 H_b v_\alpha(\hat\rho^\alpha - \mathcal{V}^\alpha)_{bc}u^\dagger_{ca}] + \cdots. \quad (18)$$

The current (18) is the most general one in the leading $1/m_c$ order of HQET and next to leading order of chiral perturbation theory. The first term is connected to the definition of the heavy meson decay constant $\langle D(p)|(\overline{q_a}c)^\mu|0\rangle = -if_D p^\mu$, where $\alpha = f_D\sqrt{m_D}$. The second and third term contribute to diagrams II and VI of Fig. 1 and diagram II of Fig. 2, where J^μ_a (18) annihilates the D meson and creates V or V_0 meson at the same time. The constants α_1 and α_2 are free parameters.

D. The choice of the parameters

We now turn to the values of the coupling constants $C_{VV\Pi}$, λ, λ', α_1 and α_2, which we need in the evaluation of the amplitudes of diagrams on Figs. 1 and 2.

The coupling $C_{VV\Pi}$ can be determined in the case of the exact $SU(3)$ flavor symmetry following the hidden symmetry approach of [30] and is found to be $|C_{VV\Pi}| = 3\tilde{g}_V^2/32\pi^2 = 0.33$. Experimentally, it can be directly determined from the $V\to PV_0\to P\gamma$ decay rates. In the following we will use the average value of $C_{VV\Pi}$, obtained from the measurements of different $V\to PV_0\to P\gamma$ decays $|C_{VV\Pi}| = 0.31$ [9], which is close to its SU(3) limit.

We determine the three parameters λ, α_1 and α_2 using three values related to the helicity amplitudes $Br = 0.048 \pm 0.004$, $\Gamma_L/\Gamma_T = 1.23\pm0.13$ and $\Gamma_+/\Gamma_- = 0.16\pm0.04$ for the process $D^+\to\overline{K}^{*0}l^+\nu_l$ [16], taken from the average of data from different experiments [14]. We get four sets of

TABLE I. The branching ratios for the Cabibbo allowed, suppressed and doubly suppressed $D \to V\mu^+\mu^-$ decays. The last column presents the experimental upper bounds [13,14], while the other columns present our theoretical predictions. The total branching ratio B_{total} containing long (Fig. 1) and short distance (Fig. 2) contributions is given in the fifth column. The third column presents only the short distance part of the branching ratio B_{SD}. The fourth column presents only the nonresonant part of the long distance contribution $B_{LD_{nonr}}$. The error bars in the table are due to the uncertainty of the model parameters expressed by the possibilities $\lambda' = \pm 0.07, \pm 0.26$ and $C_{VV\Pi} = \pm 0.31$. The branching ratios for $D \to Ve^+e^-$ obtained with the lower cut off $q^2 = (2m_\mu)^2$ (q^2 the invariant $\mu^+\mu^-$ mass) are almost exactly the same as the branching ratios for $D \to V\mu^+\mu^-$ given in this table. The second column gives the corresponding Cabibbo factors f_{Cab} in terms of the Cabibbo angle $c = \cos\theta_C$ and $s = \sin\theta_C$.

$D \to V\mu^+\mu^-$	f_{Cab}	B_{SD}	$B_{LD_{nonr}}$	B_{total}	$B_{expt.}$
$D^0 \to K^{*0}\mu^+\mu^-$	a_2c^2	0	$\leqslant 1.9\times 10^{-8}$	$[1.6-1.9]\ 10^{-6}$	$<1.18\times 10^{-3}$
$D_s^+ \to \rho^+\mu^+\mu^-$	a_1c^2	0	4.0×10^{-6}	$[3.0-3.3]\ 10^{-5}$	
$D^0 \to \rho^0\mu^+\mu^-$	$-a_2sc$	9.7×10^{-10}	$\leqslant 4.8\times 10^{-10}$	$[3.5-4.7]\ 10^{-7}$	$<2.3\times 10^{-4}$
$D^0 \to \omega\mu^+\mu^-$	$-a_2sc$	9.1×10^{-10}	$\leqslant 3.7\times 10^{-10}$	$[3.3-4.5]\ 10^{-7}$	$<8.3\times 10^{-4}$
$D^0 \to \phi\mu^+\mu^-$	a_2sc	0	$\leqslant 1.1\times 10^{-9}$	$[6.5-9.0]\ 10^{-8}$	$<4.1\times 10^{-4}$
$D^+ \to \rho^+\mu^+\mu^-$	$-a_1sc$	4.8×10^{-9}	2.7×10^{-7}	$[1.5-1.8]\ 10^{-6}$	$<5.6\times 10^{-4}$
$D_s^+ \to K^{*+}\mu^+\mu^-$	a_1sc	1.6×10^{-9}	1.5×10^{-7}	$[5.0-7.0]\ 10^{-7}$	$<1.4\times 10^{-3}$
$D^+ \to K^{*+}\mu^+\mu^-$	$-a_1s^2$	0	1.0×10^{-8}	$[3.1-3.7]\ 10^{-8}$	$<8.5\times 10^{-4}$
$D^0 \to K^{*0}\mu^+\mu^-$	$-a_2s^2$	0	$\leqslant 5.0\times 10^{-11}$	$[4.4-5.1]\ 10^{-9}$	

solutions for λ, α_1 and α_2 [16] and we choose the set, which gives the best fit with a number of the nonleptonic decays $D \to PV$, $D \to VV$ and $D \to PP$ [20]: $\lambda = -0.34 \pm 0.07$, $\alpha_1 = -0.14 \pm 0.01$, and $\alpha_2 = -0.83 \pm 0.4$.

In order to gain information on λ' we turn to an analysis of $D^{*0} \to D^0\gamma$, $D^{*+} \to D^+\gamma$ and $D_s^{*+} \to D_s^+\gamma$ decays. Experimentally, only the ratios $R_\gamma^0 = \Gamma(D^{*0} \to D^0\gamma)/\Gamma(D^{*0} \to D^0\pi^0)$ and $R_\gamma^+ = \Gamma(D^{*+} \to D^+\gamma)/\Gamma(D^{*+} \to D^+\pi^0)$ are known [14]. Taking the $R_\gamma^0 = 0.616$ and $R_\gamma^+ = 0.036$ [14], we obtain two sets of solutions for $|\lambda'/g|$ and $|\lambda/g|$, which gives two solutions for $|\lambda'/\lambda|$. The first is $|\lambda'/\lambda| = 0.77$ and the second is $|\lambda'/\lambda| = 0.21$ [9]. Taking $\lambda = -0.34$ we get four possibilities for $\lambda' = \pm 0.26, \pm 0.071$, which all have to be considered.

III. THE AMPLITUDES AND BRANCHING RATIOS FOR NINE $D \to Vl^+l^-$ DECAYS

A. The amplitudes

In this section we turn to the amplitudes and branching ratios for the nine $D \to Vl^+l^-$ decays. The interaction Lagrangians (9), (13), (14), (16), (17) and the weak currents (12), (18) provide us with the vertices in the kinematical region, where the heavy quark and chiral symmetry are good (i.e. the velocity of the heavy mesons changes only slightly in the interaction and the energy of the light mesons is small). The problem is how to extrapolate the amplitudes to the rest of the kinematical region allowed in $D \to Vl^+l^-$ decays. We assume, that the vertices do not change significantly throughout the kinematical region, which is a reasonable assumption in D decays. At the same time we use the full heavy meson propagators $1/(p^2 - m^2)$ instead of the HQET propagators $1/(2mv \cdot k)$. We account for the short life time of the intermediate neutral vector meson V_0 by using the Breit-Wigner form for the V_0 propagator

$$-i\frac{g_{\mu\nu} - \dfrac{q_\mu q_\nu}{m_{V_0}^2}}{q^2 - m_{V_0}^2 + i\Gamma_{V_0}m_{V_0}},$$

where Γ_{V_0} is the decay width of the V_0 meson and q is its momentum. Then, using the interaction Lagrangians (1), (3), (9), (13), (14), (16), (17) and the weak currents (12), (18), the calculation of the amplitudes for long distance diagrams on Fig. 1 and short distance diagrams on Fig. 2 is straightforward. The calculated amplitudes for different diagrams have in general different Lorentz structure. It is convenient to treat the amplitudes of similar Lorentz structure together. Then, the sum of the amplitudes within the model described above is given by the expression

$$\begin{aligned}\mathcal{A}[D(p) \to V(\epsilon_{(V)}, p_{(V)})l^+(p_+)l^-(p_-)] &= -\frac{G_F}{\sqrt{2}}e^2 f_{Cab}\frac{1}{q^2}\,\epsilon_{(V)\beta}\bar{u}(p_-)\gamma_\nu v(p_+) \\ &\times [\epsilon^{\mu\nu\alpha\beta}q_\mu p_\alpha A_{PC} + iA_{PV}^{\beta\nu}],\end{aligned} \tag{19}$$

where $q = p_- + p_+$ is the momentum of the intermediate virtual photon and the corresponding Cabibbo factors f_{Cab} are given in Table I. A_{PC} and $A_{PV}^{\beta\nu}$ correspond to parity conserving and parity violating amplitudes, respectively. They get contributions from different diagrams in Fig. 1 (long distance) and Fig. 2 (short distance). The short distance amplitudes A_{PC} and $A_{PV}^{\beta\nu}$ for the Cabibbo suppressed decays are

given in Appendix A. The long distance amplitudes A_{PC} and $A_{PV}^{\beta\nu}$ for the Cabibbo allowed, suppressed and doubly suppressed decays are given in Appendix B.

The decay width for $D\to Vl^+l^-$ is given by the square of the amplitude, summed over the polarizations of the three particles in the final state and integrated over the three body phase space

$$\Gamma=\frac{1}{2m_D(2\pi)^5}\sum_{polar}\int|\mathcal{A}(p_{(V)},p_+,p_-)|^2\frac{d^3p_{(V)}}{2p^0_{(V)}}\frac{d^3p_+}{2p^0_+}\times\frac{d^3p_-}{2p^0_-}\delta(p_{(V)}+p_++p_--p). \tag{20}$$

B. Discussion of the results

Firstly, we present the results for the decays with the muon final state $D\to V\mu^+\mu^-$ and we comment on the decays $D\to Ve^+e^-$ in the end. The branching ratios for the Cabibbo allowed, suppressed and doubly suppressed $D\to V\mu^+\mu^-$ decays are presented in Table I. The last column presents the experimental upper bounds [13,14]. The other columns present our theoretical predictions, where the error bars are due to the uncertainty of the model parameters λ' and $C_{VV\Pi}$, which can have any of the values $\lambda'=\pm0.07$, ±0.26 and $C_{VV\Pi}=\pm0.31$. The total branching ratio B_{total} containing long (Fig. 1) and short distance (Fig. 2) contributions is given in the fifth column. The third column presents the short distance part of the branching ratio B_{SD} calculated from Eq. (3), which is present only in the Cabibbo suppressed decays. The fourth column presents only the nonresonant part of the long distance contribution $B_{LD_{nonr}}$. This part is bigger for the charged D meson decays, where it is mainly due to diagram IV of Fig. 1. For the neutral D meson decays, diagram IV vanishes and the remaining nonresonant diagram III has a smaller amplitude, which is proportional to λ'. The parameter $\lambda'=\pm0.07,\pm0.26$ has large uncertainty and we are only able to quote the upper limit for $B_{LD_{nonr}}$.

Apart from the Cabibbo structure, the branching ratios depend mainly on whether the initial (and final) state is charged or neutral, with bigger branching ratio in the former case. We present also the distributions $(1/\Gamma_D)d\Gamma(D\to V\mu^+\mu^-)/dq^2$ as a function of q^2 (q^2 is invariant $\mu^+\mu^-$ mass) for the typical representatives of the Cabibbo allowed ($D_s^+\to\rho^+\mu^+\mu^-$ in Fig. 3 and $D^0\to\overline{K}^{*0}\mu^+\mu^-$ in Fig. 4) and suppressed ($D^0\to\rho^0\mu^+\mu^-$ in Fig. 5 and $D_s^+\to K^{*+}\mu^+\mu^-$ in Fig. 6), neutral or charged D meson decays. The short distance contribution (dot-dashed line) due to $c\to ul^+l^-$ transition is present only in the Cabibbo suppressed decays and it turns out to be much smaller than the long distance contribution. Concerning the long distance contribution, the resonant part is bigger than the nonresonant part (dashed line), except perhaps in the case of charged D meson decays at the low q^2 (see Figs. 3–6). Note, that the nonresonant LD contribution is generally

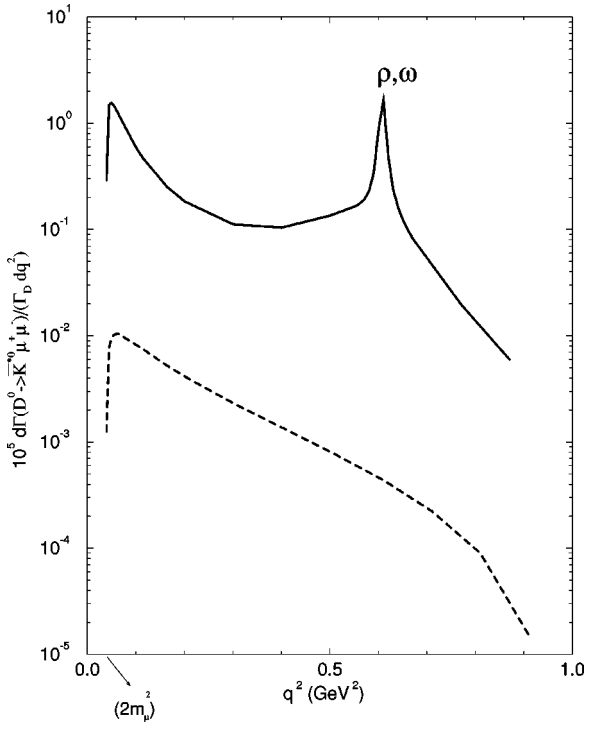

FIG. 3. The differential branching ratio $(1/\Gamma_D)d\Gamma(D^0\to\overline{K}^{*0}\mu^+\mu^-)/dq^2$ as a function of q^2 (q^2 the invariant $\mu^+\mu^-$ mass). The full line corresponds to the total branching ratio, while the dashed line represents the nonresonant long distance part. In the calculation the model parameters $\lambda'=0.26$ and $C_{VV\Pi}=0.31$ were used.

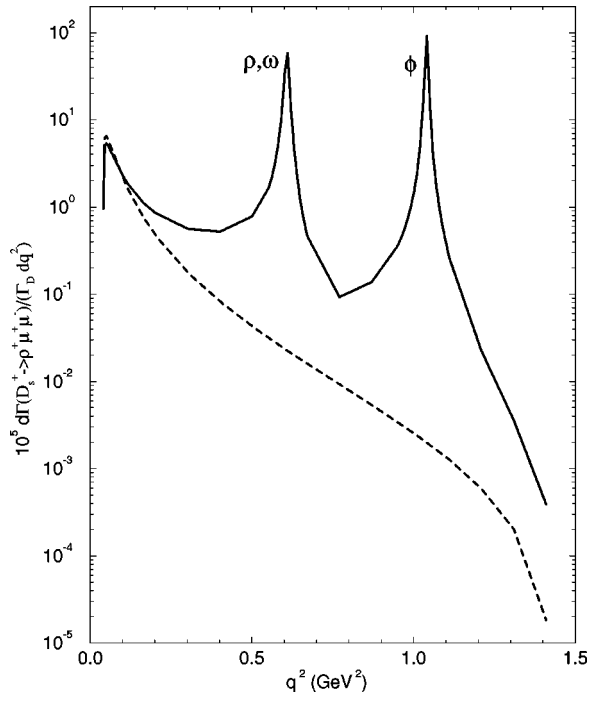

FIG. 4. The differential branching ratio $(1/\Gamma_D)d\Gamma(D_s^+\to\rho^+\mu^+\mu^-)/dq^2$ as a function of q^2 (q^2 the invariant $\mu^+\mu^-$ mass). The full line corresponds to the total branching ratio, while the dashed line represents the nonresonant long distance part. In the calculation the model parameters $\lambda'=0.26$ and $C_{VV\Pi}=0.31$ were used.

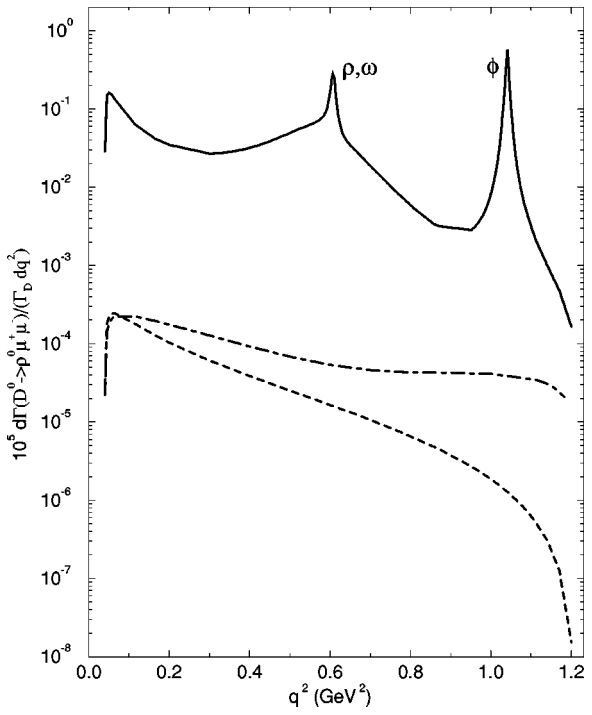

FIG. 5. The differential branching ratio $(1/\Gamma_D)d\Gamma(D^0\to\rho^0\mu^+\mu^-)/dq^2$ as a function of q^2 (q^2 the invariant $\mu^+\mu^-$ mass). The full line represents the total branching ratio, the dot-dashed line represents the short distance part, while the dashed line represents the nonresonant long distance part. In the calculation the model parameters $\lambda'=0.26$ and $C_{VV\Pi}=0.31$ were used.

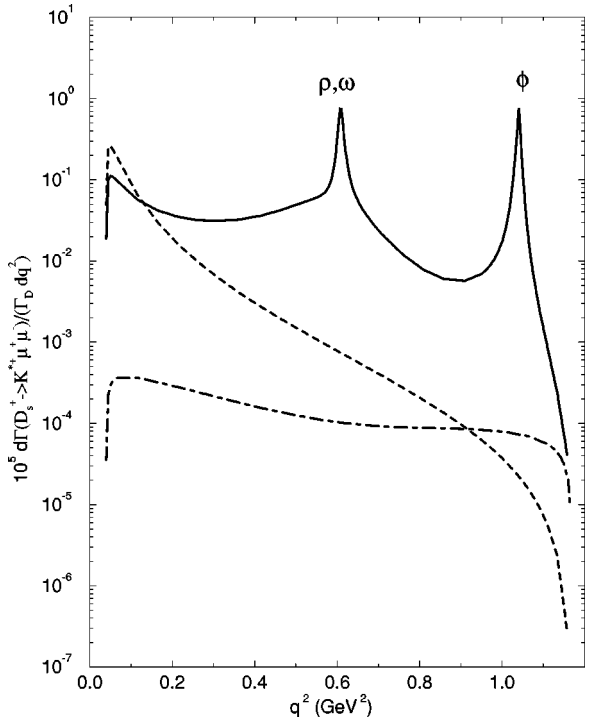

FIG. 6. The differential branching ratio $(1/\Gamma_D)d\Gamma(D_s^+\to K^{*+}\mu^+\mu^-)/dq^2$ as a function of q^2 (q^2 the invariant $\mu^+\mu^-$ mass). The full line represents the total branching ratio, the dot-dashed line represents the short distance part, while the dashed line represents the nonresonant long distance part. In the calculation the model parameters $\lambda'=0.26$ and $C_{VV\Pi}=0.31$ were used.

smaller than the resonant LD contributions even in the regions well outside the resonance peak at $q^2=m_{V_0}^2$. It is interesting to remark, that the short distance and nonresonant long distance contributions are comparable for Cabibbo suppressed neutral D meson decays $D^0\to\rho^0 l^+ l^-$ and $D^0\to\omega l^+ l^-$.

In the decays with the electron final state $D\to Ve^+e^-$ the lowest kinematically allowed q^2 is $q^2_{min}=(2m_e)^2$, which is smaller than $q^2_{min}=(2m_\mu)^2$ in the $D\to V\mu^+\mu^-$ case. In the region $q^2>(2m_\mu)^2$ the electron rates are practically equal to the muon rates. In the region $q^2<(2m_\mu)^2$, however, the rates for $D\to Ve^+e^-$ are extremely enhanced due to the photon propagator $1/q^2$. However, the region down to $q^2_{min}=(2m_e)^2$ requires a more accurate treatment of the q^2 dependence when q^2 approaches to 0, which is beyond our scope here. We have calculated the $D\to Ve^+e^-$ branching ratios with the lower cut off $q^2=(2m_\mu)^2$ and have obtained values which are very close to the $D\to V\mu^+\mu^-$ branching ratios (the $D\to V\mu^+\mu^-$ branching ratios are obtained integrating over the whole $q^2=[(2m_\mu)^2,(m_D-m_V)^2]$ region).

The Cabibbo allowed decays $D^0\to\overline{K}^{*0}\mu^+\mu^-$ and $D_s^+\to\rho^+\mu^+\mu^-$ with the predicted branching ratios of the order 10^{-6} and 10^{-5}, respectively, have the best probability for their early detection. Note that their branching ratios are not far below the present experimental upper bound.

In the Cabibbo suppressed decays, the short distance contribution due to FCNC transition $c\to ul^+l^-$ has branching ratio of order $B_{SD}\sim 10^{-10}$ and is therefore well masked by the long distance branching ratios of order 10^{-7}. Obviously, to observe the FCNC transition $c\to u$ within the standard model, one must most likely look for other possibilities. Still, new physics could enhance the SD part to be of the same order as the LD part or bigger [2,5,6]. In this case the branching ratios well above 10^{-7} for Cabibbo suppressed decays $D\to V\mu^+\mu^-$ would signal new physics. As the present experimental upper bound is much higher, these decays still contain a large discovery window.

IV. SUMMARY

We have calculated the long and short distance contributions for nine $D\to Vl^+l^-$ decays within the standard model. The short distance contribution is present only in the Cabibbo suppressed decays and is due to the flavor changing neutral transition $c\to ul^+l^-$. The long distance contribution is composed of the resonant part, which arises from the intermediate light vector meson V_0 exchange ($D\to VV_0\to V\gamma\to Vl^+l^-$), and the nonresonant part, which arises from the direct photon emission ($D\to V\gamma\to Vl^+l^-$). The branching ratios are calculated using an effective Lagrangian, which combines heavy quark symmetry and chiral perturbation theory, and are given in Table I. The most frequent decays are the Cabibbo allowed decays, which are expected at the rates, that are not much lower than the present experimental upper limit: $D_s^+\to\rho^+\mu^+\mu^-$ is expected at the branching ratio of approximately 3×10^{-5}, while $D^0\to\overline{K}^{*0}\mu^+\mu^-$ is expected at 1.7×10^{-6}. The Cabibbo suppressed decays on

the other hand, are typically expected at [3–7] 10^{-7} range for $D^0\to\rho^0(\omega)\mu^+\mu^-$ and $D_s^+\to K^{*+}\mu^+\mu^-$ decays and in the 10^{-6} range for $D^+\to\rho^+\mu^+\mu^-$ decay. Accordingly, branching ratios well above 10^{-7} for Cabibbo suppressed decays could signal new physics. In all the Cabibbo suppressed decays the short distance contribution is well masked in the standard model by the resonant long distance contribution. In the case of $D^0\to\rho^0(\omega)l^+l^-$ decays, however, the short distance contribution is of comparable size as the nonresonant long distance part.

ACKNOWLEDGMENTS

The research of S.F. and S.P. was supported in part by the Ministry of Science of the Republic of Slovenia. The research of P.S. was supported in part by the Fund for Promotion of Research at the Technion. One of us (S.F.) thanks the Physics Department at the Technion for the warm hospitality during her stay there, where part of this work was done. S.F. and S.P. are very grateful to G. Kernel and B. Keršević for many useful discussions.

APPENDIX A: THE SHORT DISTANCE AMPLITUDES

In this appendix we list the values of the Willson coefficients A_i, B_i and F_2^i in the short distance Lagrangian $\mathcal{L}_{SD}$ (3) and give the resulting short distance amplitudes A_{PC} and $A_{PV}^{\beta\nu}$ from Eq. (19).

The coefficients A_i, B_i and F_2^i have been obtained in the leading order by Inami and Lim [28] and following the notation of [4] one has

$$A_i=C_i^{box}+C_i^Z-\sin^2\theta_W(F_1^i+C_i^Z),$$

$$B_i=-\sin^2\theta_W(F_1^i+C_i^Z), \tag{A1}$$

where C_i^{box}, C_i^Z, F_1^i and F_2^i are kinematic factors, which depend on the ith-quark mass through $x_i=m_i^2/m_W^2$

$$C_i^{box}=\frac{3}{8}\left[-\frac{1}{x_i-1}+\frac{x_i\ln x_i}{(x_i-1)^2}\right]-\gamma(\xi,x_i) \tag{A2}$$

$$C_i^Z=\frac{x_i}{4}-\frac{3}{8}\frac{1}{x_i-1}+\frac{3}{8}\frac{2x_i^2-x_i}{(x_i-1)^2}\ln x_i+\gamma(\xi,x_i)$$

$$F_1^i=Q\left(\left[\frac{1}{12}\frac{1}{x_i-1}+\frac{13}{12}\frac{1}{(x_i-1)^2}-\frac{1}{2}\frac{1}{(x_i-1)^3}\right]x_i+\left[\frac{2}{3}\frac{1}{x_i-1}+\left(\frac{2}{3}\frac{1}{(x_i-1)^2}-\frac{5}{6}\frac{1}{(x_i-1)^3}+\frac{1}{2}\frac{1}{(x_i-1)^4}\right)x_i\right]\ln x_i\right)$$

$$-\left[\frac{7}{3}\frac{1}{x_i-1}+\frac{13}{12}\frac{1}{(x_i-1)^2}-\frac{1}{2}\frac{1}{(x_i-1)^3}\right]x_i-\left[\frac{1}{6}\frac{1}{x_i-1}-\frac{35}{12}\frac{1}{(x_i-1)^2}-\frac{5}{6}\frac{1}{(x_i-1)^3}+\frac{1}{2}\frac{1}{(x_i-1)^4}\right]x_i\ln x_i-2\gamma(\xi,x_i)$$

$$F_2^i=-Q\left(\left[-\frac{1}{4}\frac{1}{x_i-1}+\frac{3}{4}\frac{1}{(x_i-1)^2}+\frac{3}{2}\frac{1}{(x_i-1)^3}\right]x_i-\frac{3}{2}\frac{x_i^2\ln x_i}{(x_i-1)^4}\right)+\left[\frac{1}{2}\frac{1}{x_i-1}+\frac{9}{4}\frac{1}{(x_i-1)^2}+\frac{3}{2}\frac{1}{(x_i-1)^3}\right]x_i-\frac{3}{2}\frac{x_i^3\ln x_i}{(x_i-1)^4}. \tag{A3}$$

The summation i in $\mathcal{L}_{SD}$ (3) runs over down-like quarks (d, s and b) to which charm can couple, while $Q=-1/3$ is the corresponding charge of the intermediate quarks (we note that F_1 and F_2 have been calculated in [4] using the wrong charge $Q=2/3$). The gauge dependent term $\gamma(\xi,x_i)$ [28] cancels out in the combinations A_i, B_i and F_2^i (A1). Since the ratios x_d, x_s and x_b are of orders 10^{-8}, 10^{-6} and 10^{-3} respectively, the terms proportional to the powers of x_i can be safely neglected in (A2). With this approximation $C_i^{box}=C_i^Z=-3/8$, $F_1^i=-2\ln x_i/(9x_i-9)$ and F_2^i vanishes. In this limit the GIM cancelation occurs and we obtain

$$\sum V_iA_i=\sum V_iB_i\equiv A_{SD}=-0.065. \tag{A4}$$

Consequently, the short distance Lagrangian (3) effectively contains only the vector lepton current $\bar{l}\gamma^\mu l$ but not the axial vector $\bar{l}\gamma^\mu\gamma_5 l$ one.

The short distance $c\to ul^+l^-$ transition contributes only to the Cabibbo suppressed decays. Here we give the short distance contributions for the parity conserving A_{PC} and parity violating $A_{PV}^{\beta\nu}$ amplitudes, which are needed to calculate the Cabibbo suppressed amplitudes $\mathcal{A}[D(p)\to V(\epsilon_{(V)},p_{(V)})l^+(p_+)l^-(p_-)]$, Eq. (19). Within the model used, these amplitudes are given by the diagrams in Fig. 2:

$$A_{PC}(D^0\to\rho^0 l^+ l^-)=A_{PC}(D^0\to\omega l^+ l^-)=A_{PC}(D^+\to\rho^+ l^+ l^-)/\sqrt{2}$$

$$=A_{PC}(D_s^+\to K^{*+} l^+ l^-)/\sqrt{2}=4\,\frac{f_{D*}\lambda\tilde{g}_V}{f_{Cab}}\,\sqrt{\frac{m_{D*}}{m_D}}\frac{m_{D*}}{q^2-m_{D*}^2}\,\frac{A_{SD}q^2}{16\pi^2\,\sin^2\,\theta_W},$$

$$A_{PV}^{\beta\nu}(D^0\to\rho^0 l^+ l^-)=A_{PV}^{\beta\nu}(D^0\to\omega l^+ l^-)=A_{PV}^{\beta\nu}(D^+\to\rho^+ l^+ l^-)/\sqrt{2}$$

$$=A_{PV}^{\beta\nu}(D_s^+\to K^{*+} l^+ l^-)/\sqrt{2}=-2\,\frac{\tilde{g}_V\sqrt{m_D}}{f_{Cab}}\left[\alpha_1 g^{\beta\nu}-\alpha_2\frac{q^\beta p^\nu}{m_D^2}\right]\frac{A_{SD}q^2}{16\pi^2\,\sin^2\,\theta_W},$$

$$A_{PC}^{\beta\nu}(D^0\to\phi^0 l^+ l^-)=A_{PV}^{\beta\nu}(D^0\to\phi l^+ l^-)=0. \tag{A5}$$

The last equation is a result of Eq. (4) and the quark content of the ϕ meson. The relevant constants are presented in Appendix B.

APPENDIX B: THE LONG DISTANCE AMPLITUDES

In this appendix we give the expressions for the parity conserving A_{PC} and parity violating amplitudes $A_{PV}^{\beta\nu}$, which are needed to calculate the amplitudes $\mathcal{A}[D(p)\to V(\epsilon_{(V)},p_{(V)})l^+(p_+)l^-(p_-)]$ Eq. (19), for nine $D\to V l^+ l^-$ decays. The following amplitudes A_{PC} and $A_{PV}^{\beta\nu}$ contain the long distance resonant and nonresonant contributions coming from the diagrams on Fig. 1. The coefficients and constants needed for the evaluation of the amplitudes will be given below:

$$A_{PC}(D^0\to\overline{K}^{*0} l^+ l^-)=4J^{D^0}g_{K*}f_{D*}\,\sqrt{\frac{m_{D*}}{m_D}}\frac{m_{D*}}{m_{K*}^2-m_{D*}^2}-2K^{\overline{K}^{*0}}C_{VV\Pi}f_D m_D^2,$$

$$A_{PV}^{\beta\nu}(D^0\to\overline{K}^{*0} l^+ l^-)=M^{D^0}g_{K*}\sqrt{m_D}\left[\alpha_1 g^{\beta\nu}-\left(\alpha_1-\alpha_2\frac{q\cdot p}{m_D^2}\right)\frac{q^\beta q^\nu}{m_{V_0}^2}-\alpha_2\frac{q^\beta p^\nu}{m_D^2}\right],$$

$$A_{PC}(D_s^+\to\rho^+ l^+ l^-)=4J^{D_s^+}g_\rho f_{D_s*}\,\sqrt{\frac{m_{D_s*}}{m_{D_s}}}\frac{m_{D_s*}}{m_\rho^2-m_{D_s*}^2}-2K^{\rho^+}C_{VV\Pi}f_{D_s}m_{D_s}^2,$$

$$A_{PV}^{\beta\nu}(D_s^+\to\rho^+ l^+ l^-)=2\,f_{D_s}g_\rho\left[\frac{q^\beta p^\nu}{m_{D_s}^2-m_\rho^2}-L^{\rho^+}\frac{g^{\beta\nu}}{2}(q^2-m_\rho^2)\right]$$
$$+M^{D_s^+}g_\rho\sqrt{m_{D_s}}\left[\alpha_1 g^{\beta\nu}-\left(\alpha_1-\alpha_2\frac{q\cdot p}{m_{D_s}^2}\right)\frac{q^\beta q^\nu}{m_{V_0}^2}-\alpha_2\frac{q^\beta p^\nu}{m_{D_s}^2}\right],$$

$$A_{PC}(D^0\to\rho^0 l^+ l^-)=-4\,\frac{J^{D^0}}{\sqrt{2}}g_\rho f_{D*}\,\sqrt{\frac{m_{D*}}{m_D}}\frac{m_{D*}}{m_\rho^2-m_{D*}^2}-2K^{\rho^0}C_{VV\Pi}f_D m_D^2$$
$$-Nf_{D*}\lambda\tilde{g}_V\,\frac{a_2\,\sin\,\theta_C\,\cos\,\theta_C}{f_{Cab}}\,\sqrt{\frac{m_{D*}}{m_D}}\frac{m_{D*}}{q^2-m_{D*}^2},$$

$$A_{PV}^{\beta\nu}(D^0\to\rho^0 l^+ l^-)=M^{D^0}g_\rho\sqrt{m_D}\left[\alpha_1 g^{\beta\nu}-\left(\alpha_1-\alpha_2\frac{q\cdot p}{m_D^2}\right)\frac{q^\beta q^\nu}{m_{V_0}^2}-\alpha_2\frac{q^\beta p^\nu}{m_D^2}\right]$$
$$+\frac{N}{2}\,\tilde{g}_V\sqrt{m_D}\,\frac{a_2\,\sin\,\theta_C\,\cos\,\theta_C}{f_{Cab}}\left[\alpha_1 g^{\beta\nu}-\alpha_2\frac{q^\beta p^\nu}{m_D^2}\right],$$

$$A_{PC}(D^0\to\omega l^+l^-)=4\frac{J^{D^0}}{\sqrt{2}}g_\omega f_{D*}\sqrt{\frac{m_{D*}}{m_D}}\frac{m_{D*}}{m_\omega^2-m_{D*}^2}-2K^\omega C_{VV\Pi}f_D m_D^2$$
$$-Nf_{D*}\lambda\tilde{g}_V\frac{a_2\sin\theta_C\cos\theta_C}{f_{Cab}}\sqrt{\frac{m_{D*}}{m_D}}\frac{m_{D*}}{q^2-m_{D*}^2},$$

$$A_{PV}^{\beta\nu}(D^0\to\omega l^+l^-)=M^{D^0}g_\omega\sqrt{m_D}\left[\alpha_1 g^{\beta\nu}-\left(\alpha_1-\alpha_2\frac{q\cdot p}{m_D^2}\right)\frac{q^\beta q^\nu}{m_{V_0}^2}-\alpha_2\frac{q^\beta p^\nu}{m_D^2}\right]$$
$$+\frac{N}{2}\tilde{g}_V\sqrt{m_D}\frac{a_2\sin\theta_C\cos\theta_C}{f_{Cab}}\left[\alpha_1 g^{\beta\nu}-\alpha_2\frac{q^\beta p^\nu}{m_D^2}\right],$$

$$A_{PC}(D^0\to\phi l^+l^-)=4J^{D^0}g_\phi f_{D*}\sqrt{\frac{m_{D*}}{m_D}}\frac{m_{D*}}{m_\phi^2-m_{D*}^2}-2K^\phi C_{VV\Pi}f_D m_D^2,$$

$$A_{PV}^{\beta\nu}(D^0\to\phi l^+l^-)=M^{D^0}g_\phi\sqrt{m_D}\left[\alpha_1 g^{\beta\nu}-\left(\alpha_1-\alpha_2\frac{q\cdot p}{m_D^2}\right)\frac{q^\beta q^\nu}{m_{V_0}^2}-\alpha_2\frac{q^\beta p^\nu}{m_D^2}\right],$$

$$A_{PC}(D^+\to\rho^+l^+l^-)=4J^{D^+}g_\rho f_{D*}\sqrt{\frac{m_{D*}}{m_D}}\frac{m_{D*}}{m_\rho^2-m_{D*}^2}-2K^{\rho^+}C_{VV\Pi}f_D m_D^2$$
$$-\sqrt{2}Nf_{D*}\lambda\tilde{g}_V\frac{a_2\sin\theta_C\cos\theta_C}{f_{Cab}}\sqrt{\frac{m_{D*}}{m_D}}\frac{m_{D*}}{q^2-m_{D*}^2},$$

$$A_{PV}^{\beta\nu}(D^+\to\rho^+l^+l^-)=2f_D g_\rho\left[\frac{q^\beta p^\nu}{m_D^2-m_\rho^2}-L^{\rho^+}\frac{g^{\beta\nu}}{2}(q^2-m_\rho^2)\right]$$
$$+M^{D^+}g_\rho\sqrt{m_D}\left[\alpha_1 g^{\beta\nu}-\left(\alpha_1-\alpha_2\frac{q\cdot p}{m_D^2}\right)\frac{q^\beta q^\nu}{m_{V_0}^2}-\alpha_2\frac{q^\beta p^\nu}{m_D^2}\right]$$
$$+\frac{N}{\sqrt{2}}\tilde{g}_V\sqrt{m_D}\frac{a_2\sin\theta_C\cos\theta_C}{f_{Cab}}\left[\alpha_1 g^{\beta\nu}-\alpha_2\frac{q^\beta p^\nu}{m_D^2}\right],$$

$$A_{PC}(D_s^+\to K^{*+}l^+l^-)=4J^{D_s^+}g_{K*}f_{D_s*}\sqrt{\frac{m_{D_s*}}{m_{D_s}}}\frac{m_{D_s*}}{m_{K*}^2-m_{D_s*}^2}-2K^{K^{*+}}C_{VV\Pi}f_{D_s}m_{D_s}^2$$
$$-\sqrt{2}Nf_{D*}\lambda\tilde{g}_V\frac{a_2\sin\theta_C\cos\theta_C}{f_{Cab}}\sqrt{\frac{m_{D*}}{m_{D_s}}}\frac{m_{D*}}{q^2-m_{D*}^2},$$

$$A_{PV}^{\beta\nu}(D_s^+\to K^{*+}l^+l^-)=2f_{D_s}g_{K*}\left[\frac{q^\beta p^\nu}{m_{D_s}^2-m_{K*}^2}-L^{K^{*+}}\frac{g^{\beta\nu}}{2}(q^2-m_{K*}^2)\right]$$
$$+M^{D_s^+}g_{K*}\sqrt{m_{D_s}}\left[\alpha_1 g^{\beta\nu}-\left(\alpha_1-\alpha_2\frac{q\cdot p}{m_{D_s}^2}\right)\frac{q^\beta q^\nu}{m_{V_0}^2}-\alpha_2\frac{q^\beta p^\nu}{m_{D_s}^2}\right]$$
$$+\frac{N}{\sqrt{2}}\tilde{g}_V\sqrt{m_{D_s}}\frac{a_2\sin\theta_C\cos\theta_C}{f_{Cab}}\left[\alpha_1 g^{\beta\nu}-\alpha_2\frac{q^\beta p^\nu}{m_{D_s}^2}\right],$$

$$A_{PC}(D^+\to K^{*+}l^+l^-)=4J^{D^+}g_{K*}f_{D*}\sqrt{\frac{m_{D*}}{m_D}}\frac{m_{D*}}{m_{K*}^2-m_{D*}^2}-2K^{K^{*+}}C_{VV\Pi}f_D m_D^2,$$

$$A_{PV}^{\beta\nu}(D^+\to K^{*+}l^+l^-)=2\,f_D g_{K*}\left[\frac{q^\beta p^\nu}{m_D^2-m_{K*}^2}-L^{K^{*+}}\frac{g^{\beta\nu}}{2}(q^2-m_{K*}^2)\right]$$
$$+M^{D^+}g_{K*}\sqrt{m_D}\left[\alpha_1 g^{\beta\nu}-\left(\alpha_1-\alpha_2\frac{q\cdot p}{m_D^2}\right)\frac{q^\beta q^\nu}{m_{V_0}^2}-\alpha_2\frac{q^\beta p^\nu}{m_D^2}\right],$$

$$A_{PC}(D^0\to K^{*0}l^+l^-)=4J^{D^0}g_{K*}f_{D*}\sqrt{\frac{m_{D*}}{m_D}}\frac{m_{D*}}{m_{K*}^2-m_{D*}^2}-2K^{\bar{K}^{*0}}C_{VV\Pi}f_D m_D^2,$$

$$A_{PV}^{\beta\nu}(D^0\to K^{*0}l^+l^-)=M^{D^0}g_{K*}\sqrt{m_D}\left[\alpha_1 g^{\beta\nu}-\left(\alpha_1-\alpha_2\frac{q\cdot p}{m_D^2}\right)\frac{q^\beta q^\nu}{m_{V_0}^2}-\alpha_2\frac{q^\beta p^\nu}{m_D^2}\right]. \tag{B1}$$

Here $q=p_-+p_+$ and m_{V_0} can be approximately taken as the average of the ϕ, ω and ρ masses. The coefficients J^D, K^V, L^V, M^D and N are expressed as

$$J^{D^0}=\lambda'-\frac{\lambda\tilde{g}_V}{2\sqrt{2}}\left[\frac{g_\rho}{q^2-m_\rho^2+i\Gamma_\rho m_\rho}+\frac{g_\omega}{3(q^2-m_\omega^2+i\Gamma_\omega m_\omega)}\right], \tag{B2}$$

$$J^{D^+}=\lambda'-\frac{\lambda\tilde{g}_V}{2\sqrt{2}}\left[-\frac{g_\rho}{q^2-m_\rho^2+i\Gamma_\rho m_\rho}+\frac{g_\omega}{3(q^2-m_\omega^2+i\Gamma_\omega m_\omega)}\right],$$

$$J^{D_s^+}=\lambda'+\frac{\lambda\tilde{g}_V}{2\sqrt{2}}\frac{2g_\phi}{3(q^2-m_\phi^2+i\Gamma_\phi m_\phi)},$$

$$K^{\bar{K}^{*0}}=\left[\frac{g_\rho}{q^2-m_\rho^2+i\Gamma_\rho m_\rho}-\frac{g_\omega}{3(q^2-m_\omega^2+i\Gamma_\omega m_\omega)}+\frac{2g_\phi}{3(q^2-m_\phi^2+i\Gamma_\phi m_\phi)}\right]\frac{1}{m_D^2-m_K^2},$$

$$K^{K^{*+}}=\left[-\frac{g_\rho}{q^2-m_\rho^2+i\Gamma_\rho m_\rho}-\frac{g_\omega}{3(q^2-m_\omega^2+i\Gamma_\omega m_\omega)}+\frac{2g_\phi}{3(q^2-m_\phi^2+i\Gamma_\phi m_\phi)}\right]\frac{1}{m_D^2-m_K^2},$$

$$K^{\rho^+}=-\frac{2g_\omega}{3(q^2-m_\omega^2+i\Gamma_\omega m_\omega)}\frac{1}{m_D^2-m_\pi^2},$$

$$K^{\rho^0}=-2\sqrt{2}\,\frac{g_\rho}{q^2-m_\rho^2+i\Gamma_\rho m_\rho}\left[\frac{f_{1mix}(f_{1mix}-f_{2mix})}{m_D^2-m_{\eta^2}}+\frac{f'_{1mix}(f'_{1mix}-f'_{2mix})}{m_D^2-m_{\eta'}}\right]+\frac{\sqrt{2}}{3}\frac{g_\omega}{(q^2-m_\omega^2+i\Gamma_\omega m_\omega)}\frac{1}{m_D^2-m_\pi^2},$$

$$K^{\omega}=-2\sqrt{2}\,\frac{g_\omega}{q^2-m_\omega^2+i\Gamma_\omega m_\omega}\left[\frac{f_{1mix}(f_{1mix}-f_{2mix})}{m_D^2-m_{\eta^2}}+\frac{f'_{1mix}(f'_{1mix}-f'_{2mix})}{m_D^2-m_{\eta'}}\right]+\sqrt{2}\frac{g_\rho}{q^2-m_\rho^2+i\Gamma_\rho m_\rho}\frac{1}{m_D^2-m_\pi^2},$$

$$K^{\phi}=\frac{4}{3}\,\frac{g_\phi}{(q^2-m_\phi^2+i\Gamma_\phi m_\phi)}\left[\frac{f_{1mix}(f_{1mix}-f_{2mix})}{m_D^2-m_{\eta^2}}+\frac{f'_{1mix}(f'_{1mix}-f'_{2mix})}{m_D^2-m_{\eta'}}\right],$$

$$L^{\rho^+}=\frac{1}{q^2-m_\rho^2+i\Gamma_\rho m_\rho},$$

TABLE II. The pole masses m, decay constants f and decay widths Γ in GeV; the constants g_V in GeV^2.

H	m_H	f_H	P	m_P	f_P	V	m_V	g_V	Γ_V
D	1.87	0.21 ± 0.04	π	0.14	0.13	ρ	0.77	0.17	0.15
D_s	1.97	0.24 ± 0.04	K	0.50	/	K^*	0.89	0.19	/
D^*	2.01	0.21 ± 0.04	η	0.55	0.13 ± 0.008	ω	0.78	0.15	0.0084
D_s^*	2.11	0.24 ± 0.04	η'	0.96	0.11 ± 0.007	ϕ	1.02	0.24	0.0044

$$L^{K^{*+}}=\frac{1}{2g_{K^+}}\left(\frac{g_\rho}{q^2-m_\rho^2+i\Gamma_\rho m_\rho}+\frac{g_\omega}{3(q^2-m_\omega^2+i\Gamma_\omega m_\omega)}+\frac{2g_\phi}{3(q^2-m_\phi^2+i\Gamma_\phi m_\phi)}\right),$$

$$M^{D^0}=\frac{g_\rho}{q^2-m_\rho^2+i\Gamma_\rho m_\rho}+\frac{g_\omega}{3(q^2-m_\omega^2+i\Gamma_\omega m_\omega)},$$

$$M^{D^+}=-\frac{g_\rho}{q^2-m_\rho^2+i\Gamma_\rho m_\rho}+\frac{g_\omega}{3(q^2-m_\omega^2+i\Gamma_\omega m_\omega)},$$

$$M^{D_s^+}=-\frac{2g_\phi}{3(q^2-m_\phi^2+i\Gamma_\phi m_\phi)},$$

and

$$N=\frac{g_\rho^2}{q^2-m_\rho^2+i\Gamma_\rho m_\rho}-\frac{g_\omega^2}{3(q^2-m_\omega^2+i\Gamma_\omega m_\omega)}-\frac{2g_\phi^2}{3(q^2-m_\phi^2+i\Gamma_\phi m_\phi)}. \tag{B3}$$

The functions f_{1mix}, f'_{1mix}, f_{2mix} and f'_{2mix} are defined by

$$f_{1mix}=\frac{f_\eta}{\sqrt{8}}\left[\frac{1+c^2}{f_\eta}+\frac{sc}{f_{\eta'}}\right],$$

$$f'_{1mix}=\frac{f_{\eta'}}{\sqrt{8}}\left[\frac{sc}{f_\eta}+\frac{1+s^2}{f_{\eta'}}\right],$$

$$f_{2mix}=\frac{f_\eta}{\sqrt{8}}\left[\frac{1-5c^2}{f_\eta}-\frac{5sc}{f_{\eta'}}\right] \quad \text{and} \quad f'_{2mix}=\frac{f_{\eta'}}{\sqrt{8}}\left[\frac{-5sc}{f_\eta}+\frac{1-5s^2}{f_{\eta'}}\right], \tag{B4}$$

where $s=\sin\theta_P$, $c=\cos\theta_P$ and $\theta_P\sim 20^0$ is the $\eta-\eta'$ mixing angle. The values of the masses, decay constants and decay widths used are given in Table II.

[1] I. I. Bigi, hep-ph/9408235.
[2] J. L. Hewett, hep-ph/9505246.
[3] S. Pakvasa, hep-ph/9705397.
[4] A. J. Schwartz, Mod. Phys. Lett. A **8**, 967 (1993).
[5] G. L. Castro, R. Martinez, and J. H. Munoz, Phys. Rev. D **58**, 033003 (1998).
[6] K. S. Babu, X. G. He, X.-Q. Li, and S. Pakvasa, Phys. Lett. B **205**, 540 (1988).
[7] P. Singer and D. X. Zhang, Phys. Rev. D **55**, R1127 (1997).
[8] G. Burdman, E. Golowich, J. L. Hewett, and S. Pakvasa, Phys. Rev. D **52**, 6383 (1995).
[9] S. Fajfer and P. Singer, Phys. Rev. D **56**, 4302 (1997).
[10] S. Fajfer, S. Prelovšek, and P. Singer, hep-ph/9801279.
[11] G. Greub, T. Hurth, M. Misiak, and D. Wyler, Phys. Lett. B **382**, 415 (1996).
[12] B. Bajc, S. Fajfer, and R. J. Oakes, Phys. Rev. D **54**, 5883 (1996).
[13] CLEO Collaboration, A. Freyberger *et al.*, Phys. Rev. Lett. **76**,

3065 (1996); **77**, 2174(E) (1996); E653 Collaboration, K. Kodama *et al.*, Phys. Lett. B **345**, 82 (1995).
[14] Particle Data Group, R. M. Barnett *et al.*, Phys. Rev. D **54**, 1 (1996).
[15] M. Bauer, B. Stech, and M. Wirbel, Z. Phys. C **34**, 103 (1987).
[16] B. Bajc, S. Fajfer, and R. J. Oakes, Phys. Rev. D **53**, 4957 (1996).
[17] B. Bajc, S. Fajfer, and R. J. Oakes, Phys. Rev. D **51**, 2230 (1995).
[18] R. Casalbuoni *et al.*, Phys. Rep. **281**, 145 (1997), and references therein.
[19] P. Singer and D. X. Zhang, Phys. Rev. D **54**, 1225 (1996).
[20] B. Bajc, S. Fajfer, R. J. Oakes, and S. Prelovšek, Phys. Rev. D **56**, 7207 (1997).
[21] N. Isgur and M. B. Wise, Phys. Lett. B **232**, 113 (1989); **237**, 527 (1990).
[22] H. Georgi, Phys. Lett. B **240**, 447 (1990).
[23] M. B. Wise, Phys. Rev. D **45**, 2188 (1992).
[24] G. Burdman and J. F. Donoghue, Phys. Lett. B **280**, 287 (1992).
[25] T. M. Yan *et al.*, Phys. Rev. D **46**, 1148 (1992).
[26] R. Casalbuoni *et al.*, Phys. Lett. B **292**, 371 (1992); R. Casalbuoni *et al.*, *ibid.* **299**, 139 (1993).
[27] N. G. Deshpande, X. G. He, and J. Trampetic, Phys. Lett. B **367**, 362 (1996); G. Eilam, A. Ioanissian, R. R. Mendel, and P. Singer, Phys. Rev. D **53**, 3629 (1996).
[28] T. Inami and C. S. Lim, Prog. Theor. Phys. **65**, 197 (1981).
[29] R. Safadi and P. Singer, Phys. Rev. D **37**, 697 (1988); **42**, 1856(E) (1990); C. O. Dib, I. Dunietz, and F. J. Gilman, *ibid.* **39**, 2639 (1989).
[30] M. Bando, T. Kugo, S. Uehara, K. Yamawaki, and T. Yanagida, Phys. Rev. Lett. **54**, 1215 (1985); M. Bando, T. Kugo, and K. Yamawaki, Nucl. Phys. **B259**, 493 (1985); Phys. Rep. **164**, 217 (1988); T. Fujiwara, T. Kugo, H. Terao, S. Vehara, and K. Yamawaki, Prog. Theor. Phys. **73**, 926 (1985).